

Modulation of carrier density in ZnO nanowires without impurity doping

D. S. Kim,^{1,a)} J.-P. Richters,² R. Scholz,¹ T. Voss,² and M. Zacharias³

¹Max Planck Institute of Microstructure Physics, Weinberg 2, 06120 Halle, Germany

²Institute of Semiconductor Optics, University of Bremen, Otto-Hahn-Allee 1, D-28359 Bremen, Germany

³IMTEK, Faculty of Applied Science, Albert-Ludwigs-University Freiburg, Georges-Köhler-Allee 103, 79110 Freiburg, Germany

(Received 8 December 2009; accepted 4 March 2010; published online 24 March 2010)

ZnO nanowire based field effect transistor devices show the distinct performance depending on whether comparably oxygen-rich or oxygen-poor conditions were used for nanowire growth. Higher on-state current flows through the ZnO nanowire channel grown under oxygen-poor condition. A possible origin of this characteristic is discussed based on a photoluminescence analysis of the nanowire samples. The observed effect should be taken into account for ZnO nanowire based devices and applications. © 2010 American Institute of Physics. [doi:10.1063/1.3372632]

Semiconductor nanowires has been of continuous interest due to their potential use in electronic devices.¹ Many efforts to use nanowires as the active channels in field effect transistors (FETs) have been made.² To enhance the performance of such FETs, nanowires with atomically abrupt heterojunctions³ and core-shell structures⁴ were prepared. In addition, alternative device configurations such as wrap-gate field effect transistor⁵ are expected to reduce effectively the short channel effects and enhance the gate coupling.

ZnO with its naturally n-type conductivity is an important functional oxide material.⁶ Recently, a high performance FET based on n-type ZnO nanowires, with performance comparable to that of p-type carbon nanotube transistors has been demonstrated.⁷ However, p-type doping is still difficult to achieve even in the bulk due to the amphoteric nature of compensating native defects.⁸ After external doping, the formation energy of native donor defects is significantly reduced such that the acceptors may be fully compensated. Thus, the question of how the density of native point defects in ZnO nanowires is influenced by growth conditions is important to address.

In this work, the influence of relative content of a residual oxygen during ZnO nanowire growth on physical properties were investigated by means of electrical transport and photoluminescence measurements. ZnO nanowires grown under comparably oxygen-poor (OP) or oxygen-rich (OR) conditions showed a gate-source voltage dependence of the current flowing through the channel. The FETs based on ZnO nanowires-OP disclosed, however, a higher on-state current in transfer characteristics. We discuss the origin of this higher on-state current by taking into account the relatively higher n-type defect density in the ZnO nanowires-OP, which is attributed to the low formation energy of oxygen vacancies. Furthermore, the relative carrier densities were estimated by examining the intensity ratio between a surface exciton (SX) emission band and a bound exciton emission band.

ZnO nanowires were grown by physical vapor deposition method with Au as a nucleation agent. The quartz tube used has an outer diameter of 55 mm and a length of 650 mm. A mixture of ZnO and graphite powder with 1:1 wt %

ratio was used as source material. The tube pressure was maintained at 200 mbar under a constant Ar flow rate of 20 or 30 SCCM for wire growth. Due to the temperature gradient in our growth tube, the temperatures at the source and the nanowire collecting substrates were 920 °C and ~700 °C, respectively. The substrates were placed 12 cm away from the source boat, which was located at the center of the heating zone. Growth temperature was reached after about 25 min and maintained for 40 min. The relative content of oxygen was controlled by adjusting the Ar flow rate instead of an oxygen flow rate since wire growth events were stopped even with low oxygen flow rates of about 2 SCCM along with an Ar flow rate of 30 SCCM. This is partly due to oxidation of the graphite powder prior to catalyzing the ZnO power. Nevertheless, comparable oxygen content inside the growth tube can be controlled by the relative Ar flow rate. Wires-OP and wires-OR are used to denote ZnO nanowire samples grown under a constant Ar flow rate of 30 SCCM and 20 SCCM, respectively. It is worth noting that the flow rate of Ar is a critical factor for the growth of ZnO nanowires. The growth was strongly suppressed when an Ar flow rate of 50 SCCM was maintained. For fabrication of FETs, ZnO nanowires were deposited onto heavily doped silicon substrate capped with a 200 nm thick SiO₂ layer. The wires were located by AFM relative to predefined metal marks. Source and drain contacts were then structured by electron-beam lithography, development, thermal metal evaporation, and lift-off. A standard polymethyl methacrylate electron beam resist was used. Electrical measurements were performed under ambient conditions at room temperature. PL investigations were carried out in a liquid helium bath cryostat with temperatures ranging from 300 to 5 K. A HeCd laser with a wavelength of 325 nm and an excitation density of 100 mW/cm² was used.

Structural characterization of the ZnO nanowires grown under a different oxygen partial pressure was performed using a high-resolution transmission electron microscopy (HR-TEM). Figure 1 shows representative HRTEM images of a wire-OP [Fig. 1(a)] and a wire-OR [Fig. 1(b)] with clearly resolved lattice planes along the [0002] direction. Both, wires-OP and OR, are single crystalline without the presence of stacking faults and lattice deformations. Further, an estimated lattice distance along the [0002] direction was the same for both of wires with a value of about 0.26 nm. In

^{a)}Electronic mail: dskim@mpi-halle.de.

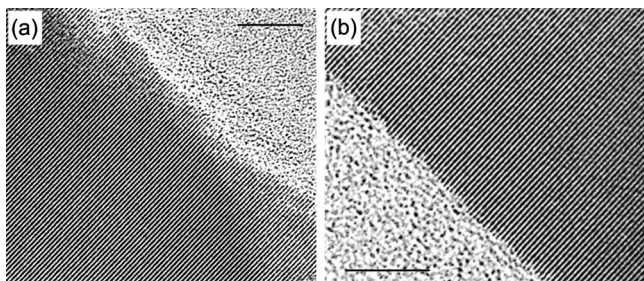


FIG. 1. HRTEM image of a wire grown under relative oxygen poor (a) and oxygen rich (b) condition. Both wires show uniform surface roughness. The scale bar is 5 nm in both (a) and (b).

order to evaluate the conductivity of the respective wires, FETs were fabricated. A schematic of device geometry and an atomic force microscopy (AFM) image of a ZnO nanowire FET is shown in Figs. 2(a) and 2(b), respectively.

Figure 3 shows the electrical characteristics of the FETs fabricated with wires-OP [Fig. 3(a)] and wires-OR [Fig. 3(b)]. The transfer characteristics indicate that both types of wires can be used for FETs devices, in that, they both show a dependence of the drain current on the gate-source voltage. However, the modulation ratio of drain current (ON/OFF ratio) for the FET based on the wire-OP is 10^7 , and 10^4 in the FET based on the wire-OR. The FET based on the wire-OP has a transconductance of $0.7 \mu\text{S}$ and a subthreshold swing of 200 mV/dec . It is noticeable, that while the current of the FET-OP at a drain-source voltage of 2 V and a gate-source voltage of 8 V [estimated from the output curve shown in Fig. 3(a), right] is about $0.6 \mu\text{A}$, it is only about $0.02 \mu\text{A}$ at the same V_{DS} and V_{GS} in the wire-OR [Fig. 3(b)]. Note that further measurements from three other wire-OP devices and a wire-OR device showed similar trends in transfer characteristics as those described above. Higher on-state current and an ON/OFF ratio of 10^7 were observed from the FET-OP devices but in the case of FET-OR device, only a few tens of on-state current (nanoampere) and an ON/OFF ratio of 10^3 were measured. Also note that the transfer characteristic of FET-OP devices measured after 54 days disclosed a large shift of the threshold voltage as well as the hysteresis.

The observed higher on-state current in the wire-OP could have multiple origins. One possible explanation for the higher on-current in the wires-OP devices with respect to that of wires-OR devices could be due to the higher density of free carriers in wires-OP.⁹ However, it is not possible to determine the doping density in wires from two-terminal measurements reliably. Thus an alternative approach was de-

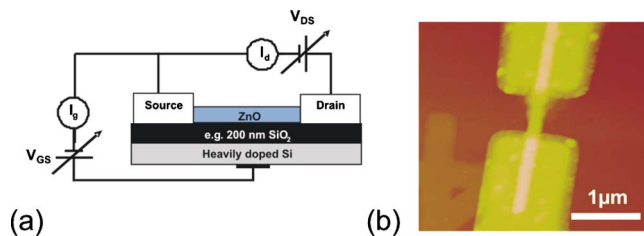


FIG. 2. (Color online) (a) Schematic depiction of the FET device and (b) AFM image of a ZnO nanowire-FET. Al was used as source and drain electrode. The electrical characteristics of the wire are shown in Fig. 3(b).

duced, using results from the photoluminescence (PL) measurements.

Recently, an enhanced SX emission in PL spectra of ZnO nanowires coated with a polymer and Al_2O_3 layers was reported.^{10,11} The coated layers act as an effective dielectric medium and screen the surface states of ZnO nanowires. This leads to a lowered effective band bending. The reduced band bending results in a high probability of forming excitons near the surface and increases the relative intensity of the SX emission with respect to the donor-bound exciton (D^0X) emission. The higher carrier concentration in ZnO nanowires may lead to a similar trend (i.e., enhanced intensity of SX compared to that of D^0X) in the PL spectra. The overlap probability of electron and hole wave functions in the vicinity of the surface should be enhanced due to the decreased extension of the depletion space charge layer, which is given by $w = (2\epsilon_s V / eN_D)^{1/2}$. N_D is the ionized donor concentration and ϵ_s is the static dielectric constant of the semiconductor. The bias V depends on the built-in potential V_{bi} , externally applied voltage V_{ext} and kT/e .¹²

Figure 4 shows the normalized near band-edge spectra of the wires-OP and the wire-OR at 9 K . The spectra of wires-OR and wire-OP are dominated not only by a sharp D^0X emission line at 3.356 eV but also show a SX band at about 3.365 eV .¹³ In addition, a broad peak at about 3.31 eV is observed. This peak noticed in phosphorus doped ZnO nanowires¹⁴ and undoped ZnO powder samples.¹⁵ Apparently, the relative intensity of the SX emission is stronger in the wires-OP compared to that of the wires-OR. Thus, one can argue that the relative carrier density in the wires-OP is higher than that in the wires-OR although quantitative values for both wires are unknown.

In ZnO, a large O-deficient nonstoichiometry is present regardless of the growth conditions.¹⁶ Such deficiency has been attributed to either an O vacancies or Zn interstitials.

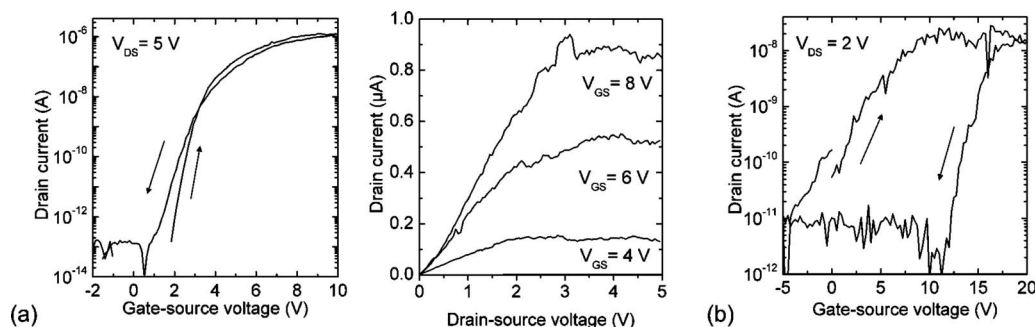


FIG. 3. (a) Representative transfer (left) and output (right) characteristics of a wire-OP. A nanowire channel in the FET has a length of $L \sim 2.2 \mu\text{m}$ and a diameter of 54 nm . (b) Representative transfer characteristics of a wire-OR with a channel length of $L \sim 0.8 \mu\text{m}$ and diameter of 86 nm . Both wires were contacted with 80 nm of aluminum and measured under ambient conditions. Arrows indicate sweep directions.

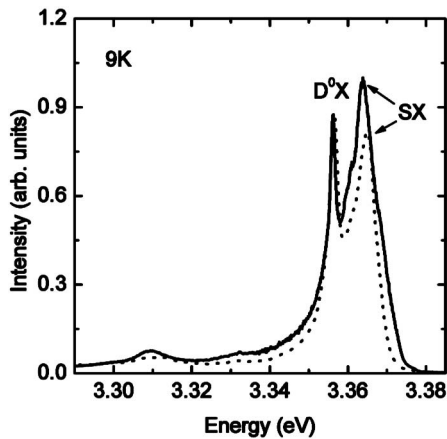


FIG. 4. Photoluminescence of ZnO nanowires grown under comparably oxygen-poor (solid) and oxygen-rich (dot) condition. The spectra have been normalized to their respective D^0X peak intensity at 3.356 eV.

Based on calculations from first-principles, however, it was predicted that the intrinsic defects only lead to moderate carrier concentrations ($\leq 10^{14} \text{ cm}^{-3}$) due to the deep level nature of the O vacancies and insufficient density of the Zn interstitials.¹⁷ Thus free carrier densities in the order of $10^{17} - 10^{19} \text{ cm}^{-3}$, which are typically observed in ZnO, cannot be directly attributed to the intrinsic point defects.¹⁸ Alternatively, persistent photoconductivity caused by the O vacancy through the optical $V_o \rightarrow V_o^+ + e$ and $V_o^+ \rightarrow V_o^{2+} + e$ excitation was suggested to account for the high carrier concentration in ZnO.¹⁷ Since oxygen vacancies can be present in concentrations of about 10^{20} cm^{-3} under equilibrium conditions the above proposed model is likely to account for the observed free carrier concentration in ZnO. The density of O vacancies can be varied by the growth conditions. For instance, the calculated defect formation energy of O vacancies is lower under oxygen-poor conditions.¹⁷ Thus, it is expected that the density of O vacancies is higher in wires-OP. In other words, the free carrier concentration in wires-OP is supposed to be higher than that in wires-OR (since typically no effort has been made to avoid visible light illumination during sample handling). It was also experimentally shown that the oxygen partial pressure during growth enables to modulate the free carrier density in ZnO films by more than three orders of magnitudes.¹⁹

We have showed that point defect concentrations in ZnO nanowires can be modified depending on growth conditions without any intentional doping. ZnO nanowires with a higher density of O vacancies showed higher on-state current in FET devices for which one possible explanation is the higher carrier concentration in the wires. Such modulation of the carrier concentration was monitored in PL spectra at low temperatures, in which the SX emission has a relative high intensity with respect to the D^0X emission. Our results indicate that the doping density can be tuned depending on growth conditions and such effects have to be considered for ZnO nanowire-based electronic and optoelectronic applications.

The authors thank Dr. R. T. Weitz at the MPI of Solid State Research for devices fabrication and electrical characterization.

- ¹L.-F. Feiner, *Nat. Nanotechnol.* **1**, 91 (2006).
- ²X. Duan, Y. Huang, Y. Cui, J. Wang, and C. M. Lieber, *Nature (London)* **409**, 66 (2001).
- ³E. Lind, A. I. Persson, L. Samuelson, and L.-E. Wernersson, *Nano Lett.* **6**, 1842 (2006).
- ⁴J. Xiang, W. Lu, Y. Hu, Y. Wu, H. Yan, and C. M. Lieber, *Nature (London)* **441**, 489 (2006).
- ⁵V. Schmidt, H. Riel, S. Senz, S. Karg, W. Riess, and U. Gösele, *Small* **2**, 85 (2006).
- ⁶C. Klingshirn, *Phys. Status Solidi B* **244**, 3027 (2007).
- ⁷S. N. Cha, J. E. Jang, Y. Choi, G. A. J. Amarantunga, G. W. Ho, M. E. Welland, and D. G. Hasko, *Appl. Phys. Lett.* **89**, 263102 (2006).
- ⁸W. Walukiewicz, *Physica B* **302-303**, 123 (2001).
- ⁹S. M. Sze, *Physics of Semiconductor Devices* (Wiley, New York, 1981).
- ¹⁰J.-P. Richters, T. Voss, L. Wischmeier, I. Rückmann, and J. Gutowski, *Appl. Phys. Lett.* **92**, 011103 (2008).
- ¹¹J.-P. Richters, T. Voss, D. S. Kim, R. Scholz, and M. Zacharias, *Nanotechnology* **19**, 305202 (2008).
- ¹²M. Grundmann, *The Physics of Semiconductors: An Introduction Including Devices and Nanophysics* (Springer, Berlin, 2006).
- ¹³L. Wischmeier, T. Voss, I. Rückmann, J. Gutowski, A. C. Mofor, A. Bakin, and A. Waag, *Phys. Rev. B* **74**, 195333 (2006).
- ¹⁴D. S. Kim, J. Fallert, A. Lotnyk, R. Scholz, E. Pippel, S. Senz, H. Kalt, U. Gösele, and M. Zacharias, *Solid State Commun.* **143**, 570 (2007).
- ¹⁵J. Fallert, R. Hauschild, F. Stelzl, A. Urban, M. Wissinger, H. Zhou, C. Klingshirn, and H. Kalt, *J. Appl. Phys.* **101**, 073506 (2007).
- ¹⁶J. H. W. de Wit, *J. Solid State Chem.* **13**, 192 (1975).
- ¹⁷S. Lany and A. Zunger, *Phys. Rev. Lett.* **98**, 045501 (2007).
- ¹⁸L. E. Halliburton, N. C. Giles, N. Y. Garces, M. Luo, C. Xu, L. Baic, and L. A. Boatner, *Appl. Phys. Lett.* **87**, 172108 (2005).
- ¹⁹G. Xiong, J. Wilkinson, B. Mischuck, S. Tuzemen, K. B. User, and R. T. Williams, *Appl. Phys. Lett.* **80**, 1195 (2002).